Nonlinear dynamo in ABC flow: The Hall effect

B. Galanti
Department of Aerospace Engineering, Israel Institute of Technology, Technion City, 32000 Haifa, Israel

N. Kleeorin
Department of Mechanical Engineering, The Ben-Gurion University of the Negev, 84105 Beer-Sheva, Israel

I. Rogachevskii
Racah Institute of Physics, The Hebrew University of Jerusalem, 91904 Jerusalem, Israel

(Received 25 April 1994; accepted 18 August 1994)

Nonlinear evolution of the magnetic field generated by a prescribed deterministic flow of a conducting fluid in form of the Arnold–Beltrami–Childress (ABC) flow is studied numerically. The nonlinearity is caused by the Hall effect. After the linear regime, the Hall term in the induction equation becomes important, leading to saturation of the magnetic field. The oscillations of the magnetic field which characterize the linear regime fade away into a steady state regime. The structure of the magnetic field can be viewed as a sum of two components: a field of the integral scale and a small-scale field. The large-scale field contains most of the energy of the system, whereas the energy of the small-scale field is very small. These results demonstrate significant difference between the actions of two types of nonlinearity in terms of the magnetic field: the Ampère force and the Hall effect. © *1994 American Institute of Physics.*

I. INTRODUCTION

Investigations of dynamo mechanisms are important from the point of view of various cosmic and laboratory applications.[1–5] Studies on the dynamo have focused on random[6–19] and deterministic[20–27] flows of conducting fluids. Many of the works are devoted to the generation of the magnetic field in prescribed deterministic flows which can be chaotic.[28–30]

However, most dynamo models are linear and predict a field that grows without limit. Hence they give no estimate of the magnitude for the generated magnetic field. To determine the magnitude of the field the nonlinear effects which limit the field growth must be taken into account. The saturation of the magnetic field may be due to two kinds of mechanisms: the first is caused by the influence of the magnetic field on the motion of the fluid, namely the action of the Ampère force in the Navier–Stokes equation.[1–4] The second is a self-induced mechanism which results in saturation of the kinematic magnetic instability (dynamo).[31,32] The latter is due to the Hall effect in two-fluid magnetohydrodynamics (MHD).[33,34] It is notable that the Ampère force yields a cubic nonlinearity in terms of the magnetic field in the induction equation, whereas the Hall effect is a quadratic. This above basic difference is essential for the energy level at saturation of the magnetic field as well as its spatial structure.

The saturation of the magnetic field by means of the Ampère force was investigated analytically and numerically for various situations. These studies can be divided into two classes: turbulent convective systems which are typical to astrophysical situations like the Sun and stars.[1–4,18,19,35,36] The other class is in simpler conditions, like considering the incompressible Navier–Stokes equation together with the induction equation in a periodic domain.[9,10,26]

An interesting investigation of the second class is a numerical study of the nonlinear saturation of the magnetic field due to interaction with a velocity field generated by a deterministic body force.[26] It was shown that when the body force acts at the integral scale of the system, the saturated magnetic field has much lower energy level than that of the velocity field. It is notable that this forcing generates an Arnold–Beltrami–Childress (ABC) flow in the absence of magnetic field and below a certain critical Reynolds number.[37,38]

The nonlinearity caused by the Hall effect in the dynamo of magnetic fluctuations excited by a random flow has been considered earlier.[31,32] A mechanism of amplification of magnetic fluctuations in the presence of zero mean field, proposed by Zeldovich,[8,5] was applied to the theory by means of a nonlinear equation derived from the induction equation; the nonlinearity was associated with the Hall effect. The local spatial distribution of the magnetic field is intermittent: the field is concentrated inside flux tubes separated by regions with weak fields. The theory yields the maximum magnitude of the magnetic field inside the flux tubes and the cross-section of the tubes.[31,32] The Hall effect is dominant in the ionosphere of Venus. In particular, on the basis of this theory[31] magnetic field observations in the ionosphere of Venus[39] are explained.

In this paper we study by means of direct numerical simulation the nonlinear saturation of the magnetic field generation caused by the Hall effect. The magnetic field is excited by a prescribed deterministic flow of a conducting fluid. Our choice as a given velocity field is the ABC flow, since its properties are well studied,[28–30,37] and leads to a generation of magnetic field.[20–23,38] We are also interested to compare our results for the Hall-nonlinearity with those obtained with the Ampère force nonlinearity.[26] Brief details of the physics of the Hall effect can be found in Sec. II. The numerical method and results of the study of the magnetic field evolution are in Sec. III.

II. THE HALL EFFECT

The evolution of magnetic field can be described by the induction equation:

$$\frac{\partial \mathbf{B}}{\partial t}=\nabla\times\left(\mathbf{v}_i\times\mathbf{B}+\frac{c}{4\pi en}\mathbf{B}\times(\nabla\times\mathbf{B})-\eta\nabla\times\mathbf{B}\right), \tag{1}$$

where $\eta=c^2/4\pi\sigma$ is the magnetic diffusivity, σ is the electrical conductivity, $\mathbf{v}_i$ is the ion velocity, e is the electron charge, n is the electron number density, and c is the light speed. The second term in Eq. (1) describes the Hall effect. The induction equation (1) is derived from the Maxwell equations and the Ohm's law.

Let us discuss the Hall effect. We consider three-fluid MHD for electrons, ions, and neutral particles. The momentum equations for electrons and ions are given by[33,34]

$$m_i n_i\left(\frac{d\mathbf{v}_i}{dt}\right)=-\nabla p_i+zen_i\mathbf{E}+\frac{zen_i}{c}(\mathbf{v}_i\times\mathbf{B})+\frac{m_e n}{\tau_{ei}}(\mathbf{v}_e-\mathbf{v}_i)+\frac{m_i n_i}{\tau_{in}}(\mathbf{u}-\mathbf{v}_i), \tag{2}$$

$$m_e n\left(\frac{d\mathbf{v}_e}{dt}\right)=-\nabla p_e-en\mathbf{E}-\frac{en}{c}(\mathbf{v}_e\times\mathbf{B})-\frac{m_e n}{\tau_{ei}}(\mathbf{v}_e-\mathbf{v}_i)+\frac{m_e n}{\tau_{en}}(\mathbf{u}-\mathbf{v}_e), \tag{3}$$

where

$$\frac{d\mathbf{v}}{dt}=\frac{\partial\mathbf{v}}{\partial t}+(\mathbf{v}\cdot\nabla)\mathbf{v},$$

$\mathbf{v}_e$, $\mathbf{v}_i$, and $\mathbf{u}$ are the electron, ion, and neutral particle velocities, respectively, m_e and m_i are the electron and ion masses, p_e and p_i are the electron and ion pressures, τ_{in}, τ_{en}, and τ_{ei} are the ion–neutral, electron–neutral, and electron–ion collision times, respectively, ze is the ion charge, n_i is the ion number density. The relationship $zn_i=n$ is due to the electrical quasineutrality of plasma, $\mathbf{E}$ is the electric field.

We neglect the inertia of electrons $m_e n(d\mathbf{v}_e/dt)$ in Eq. (3) because $m_e\ll m_i$. The Ohm's law follows from Eq. (3):

$$\mathbf{j}=\sigma\left(\mathbf{E}+\frac{1}{4\pi en}\mathbf{B}\times(\nabla\times\mathbf{B})+\frac{1}{c}\mathbf{v}_i\times\mathbf{B}+\frac{\nabla p_e}{en}\right), \tag{4}$$

where the electric current is $\mathbf{j}=en(\mathbf{v}_e-\mathbf{v}_i)$, $\nabla\times\mathbf{B}=(4\pi/c)\mathbf{j}$ and we consider for simplicity the case $\tau_{ei}\ll\tau_{en}$. So the conductivity is $\sigma=e^2 n\tau_{ei}/m_e$. The second term in the Ohm's law describes the Hall effect. The sum of Eqs. (2)–(3) yields

$$m_i n_i\left(\frac{d\mathbf{v}_i}{dt}\right)=-\nabla p+\frac{1}{c}(\mathbf{j}\times\mathbf{B})+\frac{m_i n_i}{\tau_{in}}(\mathbf{u}-\mathbf{v}_i), \tag{5}$$

where $p=p_i+p_e$, and we take into account that $m_e\ll m_i$.

The second term in Eq. (5) describes the influence of the magnetic field on the motion of plasma. It follows from Eqs. (1), (4)–(5) that this term corresponds to a cubic nonlinearity ($\sim B^3\tau_i/4\pi m_i n_i l_B$) in terms of the magnetic field in the induction equation. Here τ_i is the characteristic time of ion component of the plasma, l_B is the characteristic scale of the magnetic field variations. In contrast, the nonlinearity in the induction equation caused by the Hall effect [the second term in Eq. (1)] is a quadratic nonlinearity in terms of the magnetic field.

Now let us compare these two kind of nonlinearities. First, we consider the case $\tau_{in}\gg\tau_i$. It follows from Eq. (5) that a variation of the ion velocity δv_i under the influence of the generated magnetic field is

$$\delta v_i\sim\frac{\tau_i}{m_i n_i c}|\mathbf{j}\times\mathbf{B}|.$$

The cubic nonlinearity is not as effective as the quadratic if

$$|\delta\mathbf{v}_i\times\mathbf{B}|\ll\left|\frac{c}{4\pi en}\mathbf{B}\times(\nabla\times\mathbf{B})\right|.$$

It leads to the following criterion:

$$\omega_{Hi}\tau_i\ll 1, \tag{6}$$

where $\omega_{Hi}=eB/(m_i c)$ is the ion gyrofrequency. Note that an external force can determine the characteristic time τ_i of the ion component of plasma.

Now we study the case when the ion characteristic time τ_i is much longer than τ_{in}. Therefore, the solution of Eq. (5) is given by

$$\mathbf{v}_i=\mathbf{u}-\frac{\tau_{in}}{m_i n_i}\left(\nabla p+\frac{1}{4\pi}\mathbf{B}\times(\nabla\times\mathbf{B})\right). \tag{7}$$

For an incompressible flow $\nabla\cdot\mathbf{v}_i=\nabla\cdot\mathbf{u}=0$, the pressure can be determined from Eq. (7):

$$\Delta p=-\frac{1}{4\pi}\nabla\cdot(\mathbf{B}\times(\nabla\times\mathbf{B})).$$

It follows from (7) that the variation of the ion velocity δv_i under the influence of the generated magnetic field is

$$\delta v_i\sim\frac{\tau_{in}}{m_i n_i c}|\mathbf{j}\times\mathbf{B}|.$$

Therefore, in this case the cubic nonlinearity is not as effective as the quadratic if

$$\omega_{Hi}\tau_{in}\ll 1. \tag{8}$$

The effect of an external force $\mathbf{F}$ on plasma is reduced to an exchange of the ion velocity by a value $\tau_{in}|\mathbf{F}|/m_i n_i$. It results in the appearance of an additional external electromotive force in the induction equation (1). In the intermediate case, when $\tau_i\sim\tau_{in}$, the criteria (6) and (8) are coincided.

In this paper attention is restricted by taking into account the quadratic nonlinearity. Therefore, in the Ohm's law (4) and in the induction equation (1) we replace the ion velocity $\mathbf{v}_i$ by the velocity $\mathbf{u}$ of a prescribed deterministic flow.

III. NONLINEAR DYNAMO WITH ABC FLOW

In nondimensional form the induction equation is given by:

$$\frac{\partial\mathbf{B}}{\partial t}=\nabla\times[\mathbf{U}\times\mathbf{B}+\mathbf{B}\times(\nabla\times\mathbf{B})]+R_m^{-1}\Delta\mathbf{B}, \tag{9}$$

where coordinates and time are measured in the units $l_0 \equiv k_0^{-1} = 1$ and $t_0 = 1$, the velocity $\mathbf{U}$ is measured in the units $u_0 = l_0/t_0$, the magnetic field B is measured in units of $B_0 = 4\pi e n_e l_0^2/c t_0$, and $R_m = l_0 u_0/\eta$ is magnetic Reynolds number. Nonlinear equation (9) has been solved numerically in a 2π periodic domain.

A. The numerical method

Our numerical code utilizes a second-order Adams–Bashforth for time-marching scheme in which diffusion is treated exactly. The nonlinear terms are calculated using a Fourier (pseudo)-spectral method in space. The velocity field is given as an ABC flow:

$$\mathbf{U} = \mathbf{U}_{ABC} = (A \sin(k_0 z) + C \cos(k_0 y),$$
$$B \sin(k_0 x) + A \cos(k_0 z),$$
$$C \sin(k_0 y) + B \cos(k_0 x)) \qquad (10)$$

with $A = B = C = 1$ and the wave number $k_0 = 1$. The calculation of the nonlinear terms is the core of the computation, and shares the major part of the total computation (see the results for Navier–Stokes equation[40]). Therefore, the number of fast Fourier transforms (FFT) should be minimized. Our code requires 9 FFT's (6 inverse and 3 forward), and it seems to us to be the smallest number of FFT's required for this problem. Equation (9) is normalized so we have only the magnetic Reynolds number R_m as a control parameter.

The computations have been tested (i) against the free decay of the solution $\mathbf{B} = \mathbf{U}_{ABC}$ which has a vanishing advective term; (ii) by a verification of the results of Galloway and Frisch[23] for the linear regime (i.e., by neglecting of the Hall term).

The Hall nonlinear saturation was investigated by integration of the equation, starting from weak seed of magnetic field. We considered three different magnetic Reynolds numbers, namely $R_m = 12$, 30, and 50 (hereafter referred to as R1, R2, and R3 respectively). As follows from results[22,23] of the linear problem the magnetic field is excited by the ABC flow within two windows of the magnetic Reynolds numbers: the first one is for $9 < R_m < 17.5$ and the second one is for $R_m > 27$. Therefore, for R1, the magnetic Reynolds number belongs to the first window of linear dynamo, while R2 and R3 belong to the second window.

Since the magnetic Reynolds establishes the smallest scale of the magnetic field, the number of modes in the present simulation is as much as necessary to resolve all existing scales. In particular, the number of modes for $R_m = 12$ is 16^3 and for $R_m = 30$, 50 is 32^3.

B. Results

Figure 1 displays the time-evolution of the energy modes $E_K = \frac{1}{2}\Sigma_{|\mathbf{k}| \in C_K} |\mathbf{B}_{|\mathbf{k}|}|^2$ in spherical shells $C_K = \{K - \frac{1}{2} \leqslant |\mathbf{k}| < K + \frac{1}{2}\}$. Here $\mathbf{k}$ is the wave number and K is the number of the spherical shell. The most energetic shells are shown. At early times, starting from weak seed of magnetic field, the magnetic field, governed by the dynamo instability, grows exponentially with a growth rate found close to that of the pure linear case.[23] When the Hall term becomes important, nonlinear effects are visible and the magnetic field starts to saturate.

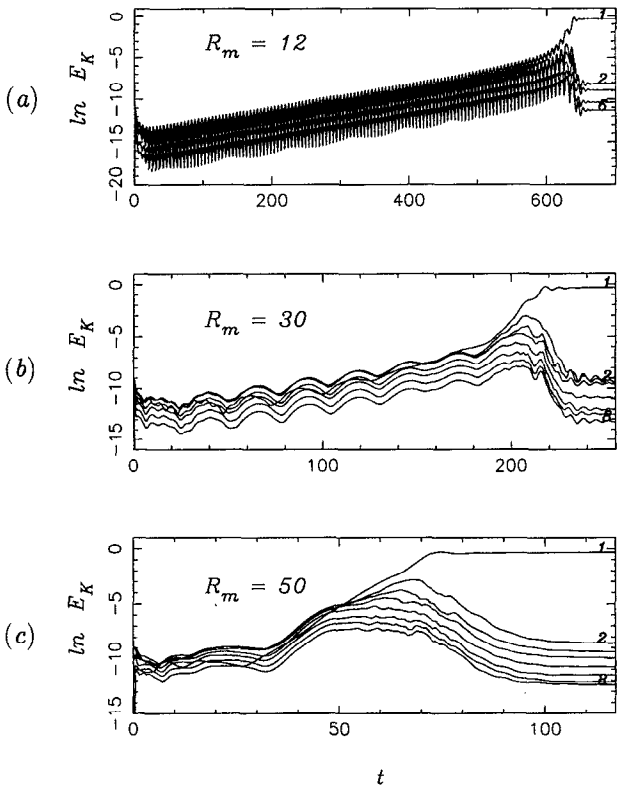

FIG. 1. The time-evolution of the magnetic energy in spherical shells around the numbers $K = 1,2,\ldots$ for the different magnetic Reynolds number: (a) $R_m = 12$; (b) $R_m = 30$; (c) $R_m = 50$.

Two important observations can at once be made: the oscillations which characterize the linear regime fade away, leading to a steady state solution; the magnetic field stabilizes at energy level of order $O(1)$ in nondimensional variables. Although the generated magnetic field is due to a deterministic velocity field, the level of the magnetic field is in agreement with that obtained for random conducting flow.[32] Inspection of the detail picture of the distribution of the energy in the different energy modes shows another important character: the energy in the first energy shell E_1 has much more significant magnitude than that of the remain E_K for $K > 1$. Furthermore, the energy distribution in the different components is found equipartitioned among the three components. Most of the energy is concentrated in modes with the wave numbers $|\mathbf{k}| = 1$ [i.e., for $\mathbf{k} = (0,0,\pm 1)$ and its cyclic permutations]. The other modes in the first shell [i.e., for $\mathbf{k} = (\pm 1, \pm 1, 0)$ and its cyclic permutations] have much lower energy. These above observed properties demonstrate the difference between the Hall-nonlinearity and that determined by the Ampère force.[26] In particular, the magnetic energy spectrum decays relatively smooth[26] and there is no energy gap between the scales as appears in the Hall-nonlinearity.

As mentioned above, the magnetic field reaches a steady

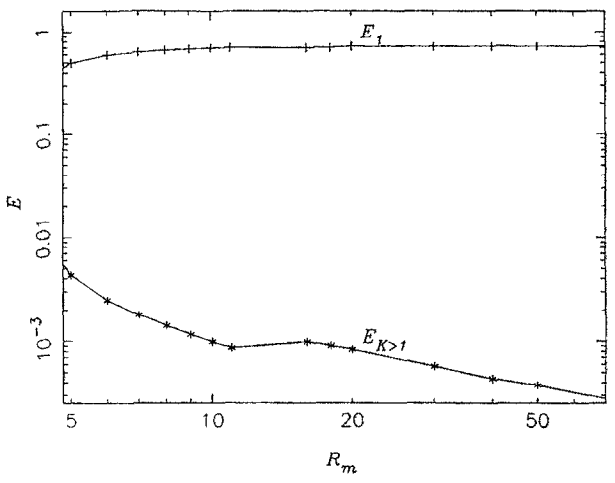

FIG. 2. The dependence of the first energy shell E_1 and the total energy in higher shells $E_{K>1}$ as function of R_m in log–log coordinates.

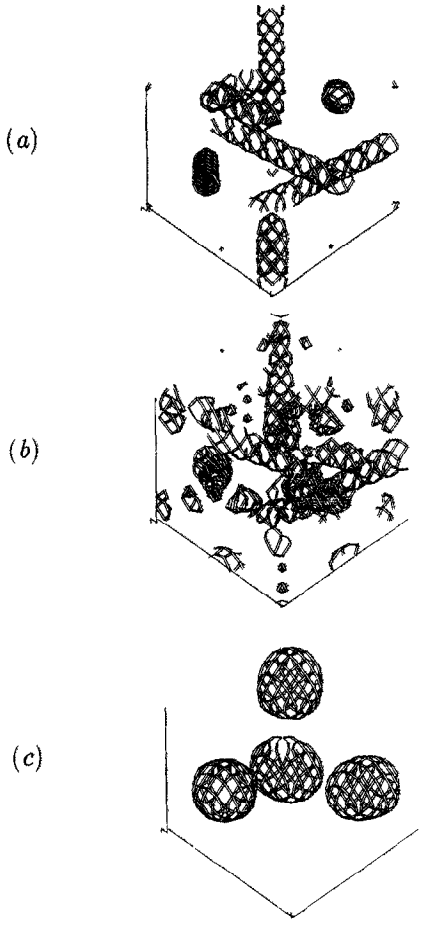

FIG. 3. The time-evolution of the magnetic field structure (contour surface of $|\mathbf{B}|$) for $R_m = 12$; (a) linear regime ($T=500$); (b) transition ($T=600$); (c) saturation ($T=700$).

state at a level of $O(1)$. In order to study the dependence of the magnetic energy with the magnetic Reynolds number the following procedure was performed: starting with a saturated magnetic field, obtained with a certain magnetic Reynolds number, we change slightly the Reynolds number and let the system evolve until the magnetic field reaches its asymptotic state. This was carried out in the interval of magnetic Reynolds numbers $0<R_m\leqslant 70$, and moreover, enabled us to even obtain magnetic fields for Reynolds numbers in between the windows of kinematic dynamo action. Figure 2 shows in log–log scales the magnetic energy in the first shell E_1 and the total energy in higher shells $E_{K>1}$ versus R_m. One can observe that the first energy shell E_1 tends to a constant level whereas $E_{K>1}$ decays almost monotonically (except of a short interval which we think is due to the different symmetries of the magnetic field). Although the range of the magnetic Reynolds number is rather limited, we find that the magnitude of the field of the smaller scales varies as $R_m^{-1/2}$. However, we cannot claim that the steady state energy level is independent of the magnetic Reynolds number for $R_m>70$, because the maximum value of R_m in our simulations is 70.

To study the evolution of the magnetic field structure as it develops from the linear regime to saturation, contour surfaces of the magnetic field $|\mathbf{B}|$ at different times are plotted (Figs. 3 and 4 for runs R1 and R3 respectively). Figures 3(a) and 4(a) show an instant during the linear regime. The four stars in Fig. 4(a)–4(c) represent the location of the four α-type stagnation points, near which the magnetic field is generated during the linear regime in cigarlike forms[23] [see Fig. 4(a)].

As the magnetic field intensifies, the configuration of the magnetic field is deformed and the so-called cigarlike structures disappear [Figs. 3(b) and 4(b)]. The configuration of the magnetic field is entirely different from that of the linear regime [Figs. 3(c) and 4(c)]. The positions of the strongest parts of the magnetic field are pushed away from the regions of the stagnation points [i.e., the strong magnetic field appears to be away from the location of the regions of the magnetic field generation in the linear stage; see Fig. 4(c)]. Note that in saturation the concentration of the magnetic field is near the regions with maximal velocity. The field displays a very regular structure. This is due to the reason that the strong part of the magnetic field is associated with the first energy mode. Note that in R1 there are four blobs of strong magnetic field whereas in R3 there are six blobs. This is due to the arrangement of the energy in the various Fourier components in the first energy shell E_1. It is also notable that during the kinematic regime, the magnetic field has some symmetries due to the velocity field[23] (depending on magnetic Reynolds number). These are broken eventually when the magnetic field saturates and new symmetries are formed (see next subsection).

Figures 5 and 6 show the contour surfaces of the magnetic field $|\mathbf{B}|$ obtained after filtering out the magnetic field associated with the first energy shell for runs R1 and R3. Figures 5(a) and 6(a) show an instant during the linear regime. The structures which appear are very similar to those obtained without filtering the magnetic field [see Figs. 3(a) and 4(a)]. This is due to the fact the growth rate of the

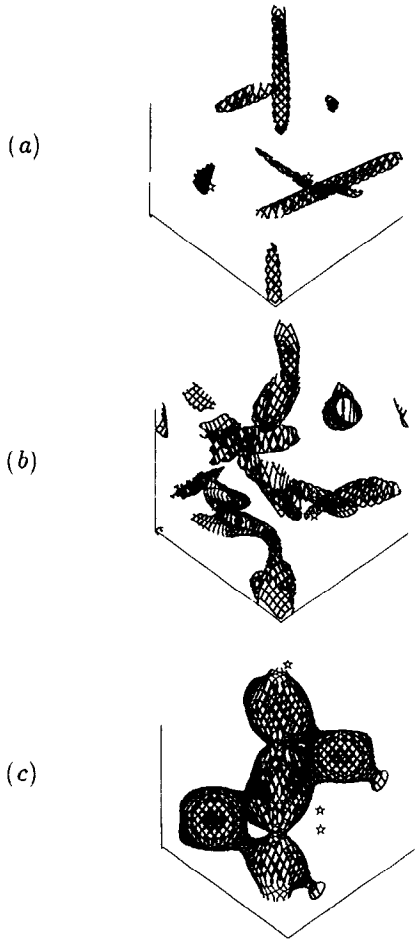

FIG. 4. The time-evolution of the magnetic field structure (contour surface of $|\mathbf{B}|$) for $R_m = 50$; (a) linear regime ($T = 37.5$); (b) transition ($T = 62$); (c) saturation ($T = 117$).

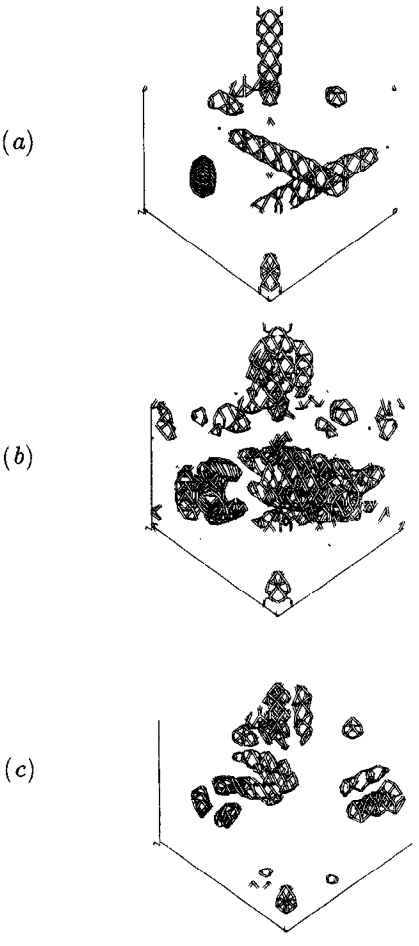

FIG. 5. The time-evolution of the magnetic field structure (contour surface of $|\mathbf{B}|$) for $R_m = 12$ for the small-scale field (the modes $K > 1$): (a) linear regime ($T = 500$); (b) transition ($T = 600$); (c) saturation ($T = 700$).

magnetic field in the linear regime is independent of the number of the shell. The next figures [5(b), 6(b)] show an intermediate instant during the nonlinear regime. It appears that the small-scale magnetic field ($K > 1$) grows in other regions, different from the locations of the original ABC stagnation points. This is due to the fact that the effective velocity field has been changed. At saturation, the structure of the magnetic field differs considerably from that of the linear regime [Figs. 5(c) and 6(c)]. However, we can see that the magnetic field is very localized and concentrates in elongated structures. As for the large-scale magnetic field, here also the small-scale magnetic field is found in saturation away from the locations of the stagnation points [see Fig. 6(c)].

C. A particular class of steady solutions for the main mode ($K = 1$)

In the previous subsection it was shown that the magnetic field reaches a steady state in which the first energy shell E_1 seems to be independent of the magnetic Reynolds number R_m. Let us construct an asymptotic solution for this mode. The steady induction equation is given by

$$\nabla \times \{\mathbf{U} \times \mathbf{B}_a + \mathbf{B}_a \times (\nabla \times \mathbf{B}_a)\} = 0. \tag{11}$$

Here we assume that for the main mode ($K = 1$) the magnetic diffusion term is negligibly small. Equation (11) is equivalent to find solution to the equation

$$(\mathbf{U} - \nabla \times \mathbf{B}_a) \times \mathbf{B}_a = \mathbf{B}_0, \tag{12}$$

where $\mathbf{B}_0 = \nabla \Phi$ and Φ is any scalar field. In order to simplify calculations (but with a loss of generality), we assume that $\mathbf{B}_0 = 0$. Having this assumption, it is easy to see that

$$\mathbf{U} - \nabla \times \mathbf{B}_a = \alpha \mathbf{B}_a \tag{13}$$

where α is any constant. Here $\mathbf{U}$ is an ABC flow as a given velocity field. It is determined by Eq. (10), where A, B, and C are arbitrary coefficients. After some algebra we find a class of steady solutions with the following form:

$$
\begin{aligned}
\mathbf{B}_a = & [A_1 \sin(k_0 z) + A_2 \cos(k_0 z) + C_2 \sin(k_0 y) \\
& + (C - C_1)\cos(k_0 y)\ , \\
& B_1 \sin(k_0 x) + B_2 \cos(k_0 x) + A_2 \sin(k_0 z) \\
& + (A - A_1)\cos(k_0 z)\ , \\
& C_1 \sin(k_0 y) + C_2 \cos(k_0 y) + B_2 \sin(k_0 x) \\
& + (B - B_1)\cos(k_0 x)]\ , \qquad (14)
\end{aligned}
$$

where A_1, A_2, B_1, B_2, C_1, and C_2 are arbitrary coefficients. Here we take into account that most of magnetic energy is concentrated in modes with the wave numbers $|\mathbf{k}| = 1$ [i.e., for $\mathbf{k} = (0,0,\pm 1)$ and its cyclic permutations] and the other modes in the first shell [i.e., for $\mathbf{k} = (\pm 1, \pm 1, 0)$ and its cyclic permutations] have much lower energy (see the results of the numerical simulations in Sec. III B). To obtain a specific solution, it is necessary to find the unknown coefficients in Eq. (14). They can be determined by means of comparison with the numerical solution for a given R_m. In that sense, the obtained asymptotic solution can be regarded as a R_m dependent solution for the main mode ($K = 1$).

The assumptions above were verified numerically. The first one, that the diffusion is negligible, was checked by computing the PDF of the ratio $q = R_m^{-1}|\Delta \mathbf{B}|/|\nabla \times (\mathbf{U} \times \mathbf{B}_a)|$. Figure 7(a) shows the distribution of the ratio q for $R_m = 50$. It is clear that the contribution of the diffusive term is very small. Next assumption, namely that $|\mathbf{B}_0| = 0$, was checked by the calculation of LHS of Eq. (12). Figure 7(b) shows the PDF of the LHS of Eq. (12). It indicates that $\mathbf{B}_0$ can be regarded negligible small. Finally, we verified if α is constant. Figure 7(c) shows the PDF of α. It confirms that α is nearly constant. Similar results are found for $R_m = 12$ and 30.

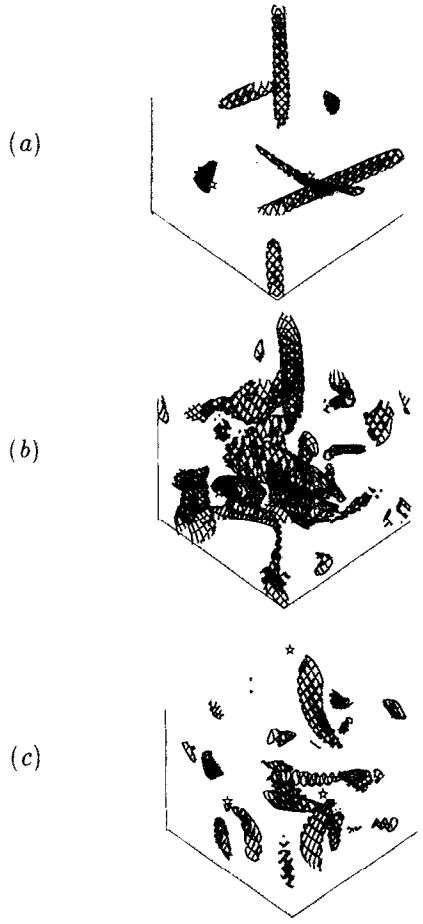

FIG. 6. The time-evolution of the magnetic field structure (contour surface of $|\mathbf{B}|$) for $R_m = 50$ for the small-scale field (the modes $K > 1$) : (a) linear regime ($T = 37.5$); (b) transition ($T = 62$); (c) saturation ($T = 117$).

IV. DISCUSSION

This paper presents numerical simulations of the magnetic field evolution excited by a prescribed deterministic ABC flow of a conducting fluid. We have found that the Hall nonlinearity results in a saturation of the growth of the magnetic field. The magnetic field in the saturation in all considered cases (for $R_m < 70$) reaches a steady state with the energy level and seems to be independent of the magnetic Reynolds number R_m.

Moreover, the magnetic field structure may be regarded as composed from two components: a field of the integral scale and a small-scale field. Most of the magnetic energy is concentrated in the former, whereas in the latter it is much smaller. Comparison with saturation obtained by Ampère force[26] shows that there is no energy gap between the scales as appear in the Hall-nonlinearity. These results demonstrate a difference between the actions of two types of nonlinearity in terms of the magnetic field: the Ampère force and the Hall effect. In the case of Ampère nonlinearity, the Ampère force changes the hydrodynamic flow of the conducting fluid. As to the Hall nonlinearity, it does not affect the hydrodynamic flow. It only changes the topology of the field and electric current. The maximum of the field in saturation is far from the region of the generation.

In the case of the Hall-nonlinearity we have obtained that in nondimensional variables the magnetic energy is of the order of the hydrodynamic energy in the saturation. However, in dimensional variables the ratio of magnetic $W_B = B^2/8\pi$ and hydrodynamic $W_u = \rho \mathbf{u}^2/2$ energy is given by

$$
\frac{W_B}{W_u} \sim \left(\frac{\omega_{pi} l_0}{c}\right)^2 .
$$

Here $\omega_{pi} = (4\pi z^2 e^2 n/m_i)^{1/2}$ is the plasma frequency of ions. It is seen from here that the level of generated magnetic field depends on both the plasma density and the size of the system in the case of the Hall-nonlinearity. Substitution of the obtained magnitude of the magnetic field in the criterion (6) yields

$$
\left(\frac{\omega_{pi} l_0}{c}\right)^2 \left(\frac{\tau_i}{t_0}\right) \ll 1 .
$$

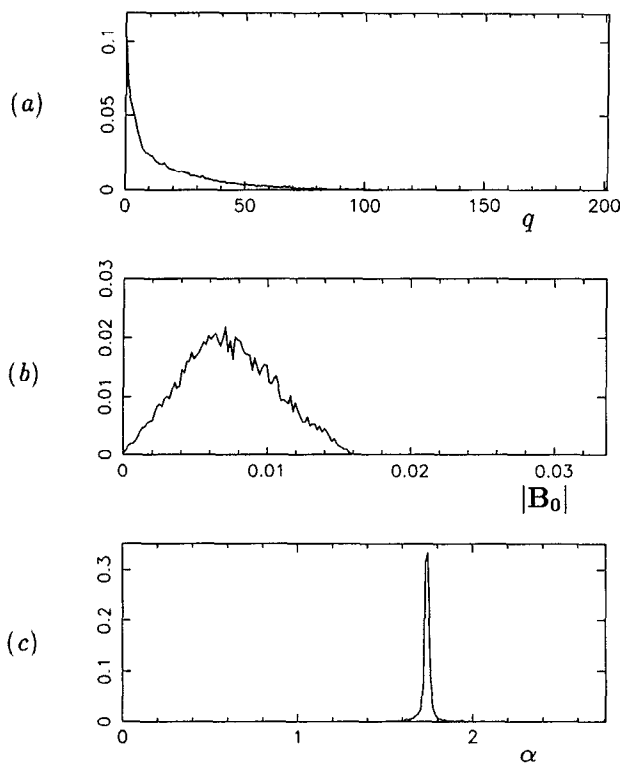

FIG. 7. Numerical verification of the assumptions for the particular class of steady solutions (for $R_m=50$): (a) the PDF of the ratio $q=R_m^{-1}|\Delta\mathbf{B}|/|\nabla\times(\mathbf{U}\times\mathbf{B}_a)|$; (b) the PDF of $|\mathbf{B}_0|$; (c) the PDF of α.

It follows from here that when $\tau_i \ll t_0$ and $\tau_{in} \ll t_0$ (see Sec. II) the magnetic energy can be of the order of the hydrodynamic energy in the saturation.

We have found that the spatial distribution of the small-scale field is intermittent: the field is concentrated within magnetic structures separated by the regions with very small field. The length of the structures is of the scale of the system. The properties of the small-scale field seem to be similar to that of magnetic fluctuations with zero mean field excited by a random flow of conducting fluid.[5,11,32]

Future studies will be concentrated on the evolution of the magnetic field in random and deterministic flow after accounting for the cubic nonlinearity (two-fluid magnetohydrodynamics) for the higher magnetic Reynolds number.

ACKNOWLEDGMENTS

We have benefited from stimulating discussions with B. Meerson who initiated this work. We thank A. Gilbert for comments on the manuscript. The useful criticism made by the anonymous referees is gratefully acknowledged.

The work was supported in part by the Israel Ministry of Science.

[1]H. K. Moffatt, *Magnetic Field Generation in Electrically Conducting Fluids* (Cambridge University Press, New York, 1978).
[2]E. Parker, *Cosmical Magnetic Fields* (Oxford University Press, New York, 1979), and references therein.
[3]F. Krause and K. H. Rädler, *Mean-Field Magnetohydrodynamics and Dynamo Theory* (Pergamon, Oxford, 1980), and references therein.
[4]Ya. B. Zeldovich, A. A. Ruzmaikin, and D. D. Sokoloff, *Magnetic Fields in Astrophysics* (Gordon and Breach, New York, 1983).
[5]Ya. B. Zeldovich, A. A. Ruzmaikin, and D. D. Sokoloff, *The Almighty Chance* (World Scientific, Singapore, 1990).
[6]R. H. Kraichnan and S. Nagarajan, Phys. Fluids **10**, 859 (1967).
[7]A. P. Kazantsev, Sov. Phys. JETP **26**, 1031 (1968).
[8]S. I. Vainshtein and Ya. B. Zeldovich, Sov. Phys. Usp. **15**, 159 (1972).
[9]M. Meneguzzi, U. Frisch, and A. Pouquet, Phys. Rev. Lett. **41**, 1060 (1981).
[10]J. Leorat, U. Frisch, and A. Pouquet, J. Fluid Mech. **104**, 419 (1981).
[11]S. A. Molchanov, A. A. Ruzmaikin, and D. D. Sokoloff, Sov. Phys. Usp. **28**, 307 (1985).
[12]N. Kleeorin, I. Rogachevskii, and A. Ruzmaikin, Sov. Phys. JETP **70**, 878 (1990).
[13]F. Cattaneo and S. I. Vainshtein, Astrophys. J. **376**, L21 (1991).
[14]R. M. Kulsrud and S. W. Anderson, Astrophys. J. **396**, 606 (1991).
[15]S. I. Vainshtein and R. Rozner, Astrophys. J. **376**, 199 (1991).
[16]A. Nordlund, A. Brandenburg, R. L. Jennings, M. Rieutord, J. Ruokolainen, R. F. Stein, and I. Tuominen, Astrophys. J. **392**, 647 (1992).
[17]N. Kleeorin and I. Rogachevskii, Phys. Rev. E. **50**, 2716 (1994).
[18]A. Brandenburg, R. L. Jennings, A. Nordlund, M. Rieutord, R. F. Stein, and I. Tuominen, "Magnetic structures in a dynamo simulations," to appear in J. Fluid Mech.
[19]A. Brandenburg, F. Krause, A. Nordlund, A. Ruzmaikin, R. F. Stein, and I. Tuominen, "On the magnetic fluctuations produced by a large-scale magnetic field," submitted to Astrophys. J.
[20]S. Childress, J. Math. Phys. **11**, 3063 (1970).
[21]V. I. Arnol'd, Ya. B. Zeldovich, A. A. Ruzmaikin, and D. D. Sokoloff, Sov. Phys. JETP **54**, 1083 (1981).
[22]V. I. Arnol'd and E. I. Korkina, Vestn. Mosk. Univ. Mat. Mekh. **3**, 43 (1983) (in Russian).
[23]D. J. Galloway and U. Frisch, Geophys. Astrophys. Fluid Dyn. **36**, 53 (1986).
[24]J. M. Finn and E. Ott, Phys. Fluids **31**, 2992 (1988); Phys. Fluids B **2**, 916 (1990).
[25]A. D. Gilbert and S. Childress, Phys. Rev. Lett. **65**, 2133 (1990).
[26]B. Galanti, P. L. Sulem, and A. Pouquet, Geophys. Astrophys. Fluid Dyn. **66**, 183 (1992).
[27]Y. T. Lau and J. M. Finn, Phys. Fluids B **2**, 916 (1993).
[28]V. I. Arnol'd, C. R. Acad. Sci. Paris **261**, 17 (1965).
[29]M. Henon, C. R. Acad. Sci. Paris **262**, 312 (1966).
[30]G. M. Zaslavskii, R. Z. Sagdeev, and A. A. Chernikov, Sov. Phys. JETP **67**, 270 (1988).
[31]N. Kleeorin, I. Rogachevskii, and A. Eviatar, J. Geophys. Res. A **99**, 6475 (1994).
[32]N. Kleeorin and I. Rogachevskii, Phys. Rev. E **50**, 493 (1994).
[33]S. I. Braginskii, in *Reviews of Plasma Physics*, edited by M. A. Leontovich (Consultants Bureau, New York, 1965), Vol 1, p. 205.
[34]F. F. Chen, *Introduction to Plasma Physics and Controlled Fusion* (Plenum, New York, 1984).
[35]N. Kleeorin, I. Rogachevskii, and A. Ruzmaikin, "Solar irradiance variations and nonlinear mean field dynamo," to appear in Solar Phys. (1994).
[36]N. Kleeorin, I. Rogachevskii, and A. Ruzmaikin, "Magnitude of dynamo-generated magnetic field in solar-type convective zones," to appear in Astron. Astrophys. (1994).
[37]T. Dombre, U. Frisch, J. M. Green, M. Henon, A. Mehr, and A. M. Soward, J. Fluid Mech. **167**, 353 (1986).
[38]D. J. Galloway and U. Frisch, J. Fluid Mech. **180**, 557 (1987).
[39]C. T. Russell and R. C. Elphic, Nature **279**, 616 (1979).
[40]C. Basdevant, J. Comput. Phys. **50**, 209 (1983).